Light and electron microscopy of apoptotic DNA fragmentation

L. Biagiotti,[1] P. Ferri,[1] A. D'Emilio,[1] M.B.L. Rocchi,[2] E. Falcieri,[1,3] S. Burattini[1]

[1]Istituto di Scienze Morfologiche e [2]Istituto di Biomatematica, Università degli Studi di Urbino "Carlo Bo"; [3]Istituto di Genetica Molecolare,CNR, Istituti Ortopedici Rizzoli, Bologna, Italy

Corresponding author: Elisabetta Falcieri,
Istituto di Scienze Morfologiche, Università degli Studi di Urbino, Campus Scientifico
Località Crocicchia 61029 Urbino (PU)
Tel. +39.0722.304284 Fax +39.0722.304244
E-mail: elisabetta.falcieri@uniurb.it

Summary

One of the most known apoptotic markers is DNA fragmentation. The cell initially produces large 50-300kbp fragments and, successively, oligonucleosimic ones.

However, apoptosis without DNA fragmentation, with the typical apoptotic features, such as chromatin condensation and micronuclei, has been reported.

In this work we have investigated the relationship between apoptotic morphology and the underlying DNA behaviour in two different cell lines (U937 and Molt-4), undergoing apoptosis after UVB irradiation or staurosporine treatment.

TUNEL reaction was utilized both in fluorescence (by FITC) and transmission electron microscpy (by colloidal gold). While the first only highlights apoptosis presence or absence in cells, the second reveals a precise localization of DNA break points, clearly identified by colloidal gold, in diffuse or dense chromatin.

Colloidal gold particles density was evaluated in the different experimental conditions and was correlated to DNA fragmentation patterns.

Keywords: apoptosis, DNA fragmentation, TUNEL/LM, TUNEL/TEM, U-937, Molt-4, UVB, staurosporine.

Introduction

Apoptosis, also called "suicide program", is a common cell phenomenon occuring during development and required for homeostasis of multicellular organisms [1]. Moreover, apoptosis is also activated by some pro-apoptotic physical (radiations) and chemical (staurosporine, cisplatin, camptothecin, etoposide, methotrexate, hydrogen peroxide and others) agents.

The process can be initiated by two distinct pathways: an extrinsic or an intrinsic one. The first involves cell surface death receptors (Fas/Fas-L or others) while in the second mitochondria play a crucial role [2].

Both conditions produce a sequential activation of different cysteine proteases (caspase cascade) and, consequently, specific morphological changes, such as chromatin condensation, nuclear breakdown, cell shrinkage, membrane blebbing and, later, apoptotic bodies [3, 4]. These undergo phagocytosis *in vivo* while a secondary necrosis takes place *in vitro*.

A biochemical hallmark of apoptosis is DNA fragmentation [5, 6]. This process is characterized by two steps: the formation of larger DNA fragments (50-300 kbp) and, mostly, by the subsequent formation of oligonucleosomes (180 bp) [7]. DNA breaks are produced by two specific caspase3-activated endonucleases, called DNase I and DNase II, that yield free 3'-OH ends [8].

However, apoptosis without DNA fragmentation, at least the oligonucleosomic one, in the presence of typical chromatin condensation, has been reported [9-12].

In this work we have investigated the behaviour of two different cell lines (U937 and Molt-4) exposed to UVB or incubated with staurosporine. The

first trigger induces production of reactive oxygen species, determining irreversible and reversible structural and functional changes of cells and their organelles [13]. Staurosporine is a PKC inhibitor.

Apoptosis was investigated by conventional electron microscopy, by TUNEL reaction and by a modified TUNEL technique, utilizing colloidal gold. The density of gold particles, which identify double strand DNA breaks, was correlated to DNA cleavage patterns.

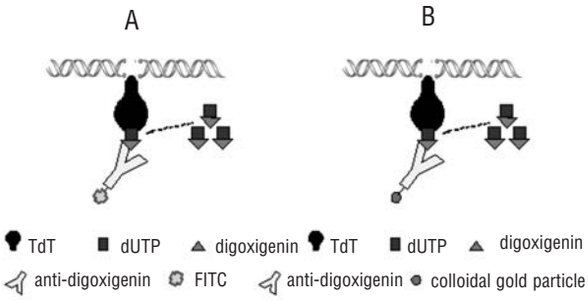

Figure 1. Schematic rapresentation of TUNEL/LM (A) and TUNEL/TEM (B) technique.

Materials and methods

Cell lines and culture conditions

U937 myelomonocytic human leukaemia cells and Molt-4 T-lymphoblastoid cells were grown in RPMI 1640 supplemented with 10% heat-inactivated fetal bovine serum, 2 mM glutamine, 25 mM HEPES pH 7.5, and 1% antibiotics. They were maintained at 37°C in humidified air with 5% CO_2 and cell viability were assessed by trypan blue exclusion test (14, 15).

Induction of apoptosis

U937 and Molt-4 cells ($1x10^6$ cells/mL) were exposed for 30 min to a 302-nm UVB transilluminator source at a distance of 3-5 cm. Cells cultures were then successively incubated for 4,6,8,10 or 24 hr at 37°C in 5% CO_2. Staurosporine, an inhibitor of protein kinases C, were dissolved in ethanol and supplied 200 nM both to U937 and Molt-4 cells for 24h.

TUNEL/LM

$1x10^5$ cells/mL were spun on poly-L-lysine-coated slides at 900 rpm for 10 min. They were washed and fixed with 4% paraformaldehyde in PBS (pH 7.4) for 30 min at room temperature, rinsed with PBS and permeabilized with a mixture 2:1 of ethanol and acetic acid for 5 min at -20°C.

For the TUNEL technique, all reagents were part of a kit (Apoptag Plus, D.B.A., Oncor) and procedures were carried out according to the manufacturer's instructions [1, 18]. Cells were treated with TdT buffer, containing the digoxigenin-conjugated dUTP, for 10 min at room temperature.

Afterwards, cells were incubated with the reaction buffer containing the TdT enzyme for 1h at 37°C in a humified chamber. The reaction was blocked by the stop buffer for 10 min. Cells were incubated with a FITC-conjugated anti-digoxigenin antibody for 30 min at room temperature (Figure 1A). Finally slides were mounted with an antifading medium. Specimens were observed and photographed with a VANOX (Olympus Italia s.r.l., MI) fluorescence microscope.

TUNEL/TEM

For the ultrastructural analysis, the TUNEL assay was modified according to Lossi and coworkers (Neuroscience, 2002). Cells were fixed with a mixture of 2% glutaraldehyde and 1% paraformaldehyde in Sorensen buffer (0.1M, pH 7.4) for 1h, post-fixed with 1% OsO_4 in the same buffer for 1h and embedded in araldite. The TUNEL procedure was carried out on thin sections, collected on nickel grids. Reagents were part of the same kit (Apoptag Plus, D.B.A., Oncor). Thin sections were treated with TdT buffer for 5 min at room temperature and then incubated with the TdT reaction buffer for 2h at 37°C in an humid chamber.The reaction was blocked by the stop buffer for 10 min. After rinsing with 1% bovine serum albumin in TBS buffer (Tris/HCl 0,02M, pH 8,2), the sections were incubated with 10 nm particle colloidal gold-conjugated anti-digoxigenin antibody (D.B.A., Aurion, 1:40) in TBS buffer for 1h at 37°C. Sections were rinsed with 1% BSA in TBS buffer followed by distilled water and post-fixed with glutaraldehyde 2.5% in cacodylate buffer 0.1 M for 10 min (Figure 1 B). Negative controls were carried out without TdT enzyme. Finally, sections were stained with uranyl acetate and lead citrate and analysed with a Philips CM10 electron microscope.

Colloidal gold particle statistical evaluation

For the quantitative analysis, electron micrographs at 100.000x final magnification were analyzed.

For each experiment, 2-3 grids, from various resin-embedded specimens, were observed, and for each grid about 10-15 micrographs were selected. Areas of exclusively decondensed and dense chromatin (i.e. euchromatin *vs* heterochromatin in control cells and diffuse vs compact chromatin in apoptotic ones) were selected and the gold particles were counted. For each experimental condition a total area of 3000 μm^2 was examined. The gold particle number of each area was divided by the size of the corresponding area to obtain the gold particles density. Density values for each area were averaged.

Statistical analysis

The differences among the groups were evaluated by a 4-way Anova test. Values of $p<0.05$ were considered statistically significant.

Results

Both U937 and Molt-4 cells are TUNEL/LM negative in control condition (Figure 2 A,B). On the contrary, TUNEL/TEM shows a weak labelling, mainly placed under nuclear envelope and in heterocromatin areas (Figure 3 C,D). This phenomenon [20] is certainly correlated to the higher resolution power of TEM and colloidal gold techniques respect LM methods. Moreover, many studies have described DNA break points produced by endogenous and environmental DNA-damaging agents.

After UVB exposure TUNEL/LM (Figure 3 A-C) highlights a strong positivity, particulary in U937 cells, with numerous micronuclei (Figure 3 B,C).

TUNEL/TEM reveals a specific localization of DNA break points (Figure 3 D-F). While cytoplasm is negative, an intense labelling appears in apoptotic dense chromatin, located at nuclear periphery

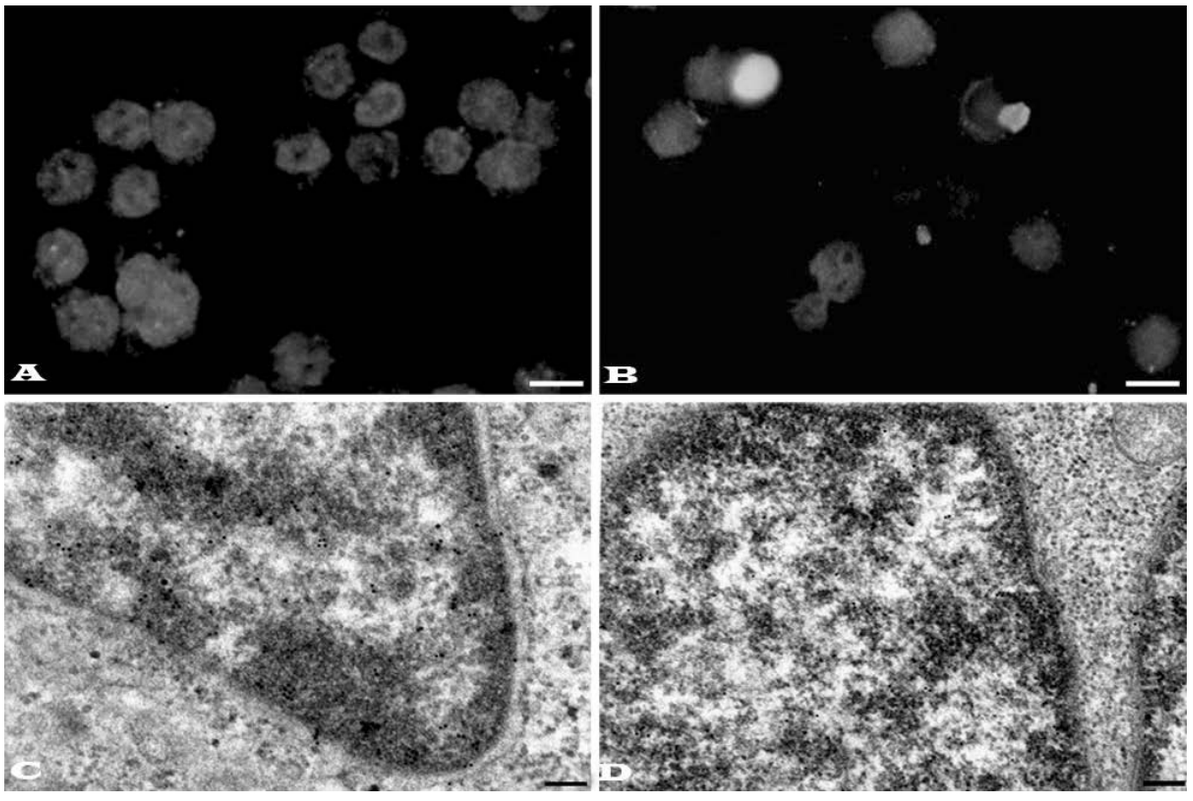

Figure 2. U937 (A,C) and Molt-4 (B,D) control cells, after TUNEL/LM (A,B) and TUNEL/TEM. (C,D). TUNEL/LM-negative cells show, after TUNEL/TEM, a weak staining, mainly located under nuclear envelope and in heterochromatin areas. A,B bar=25 µm; C,D bar=0,2 µm.

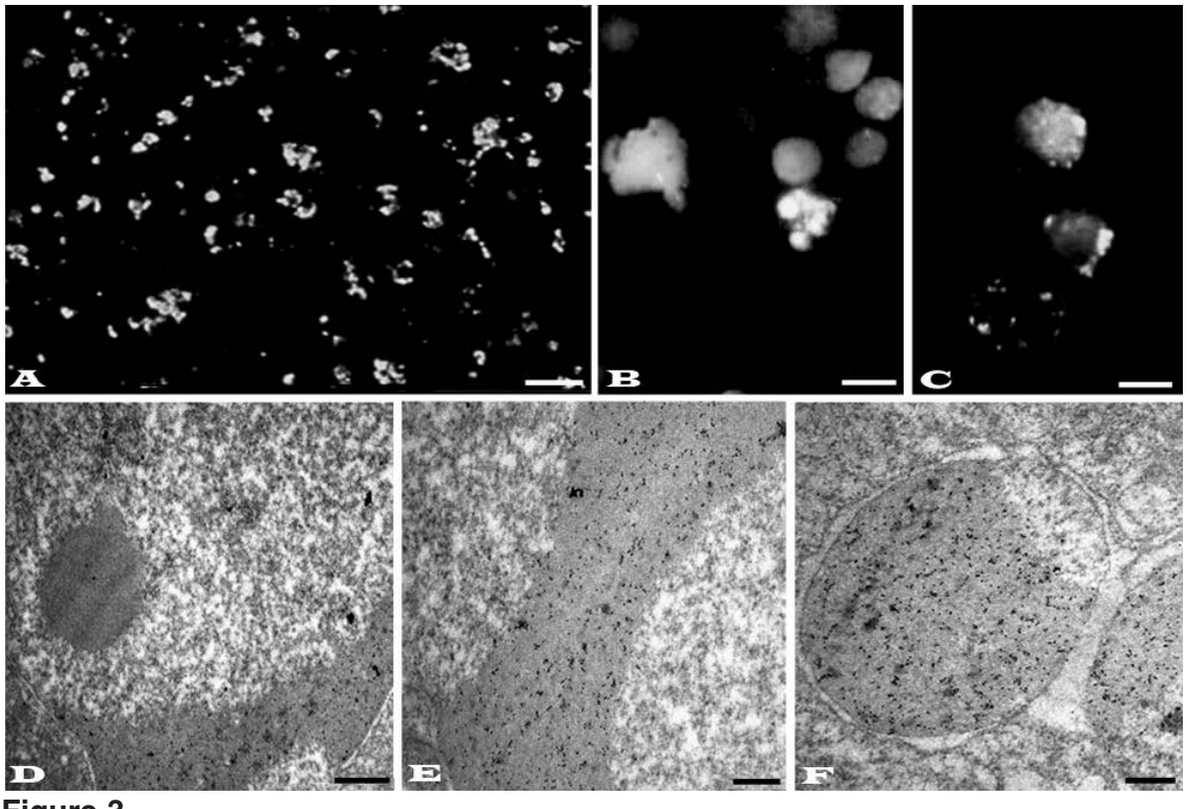

Figure 3

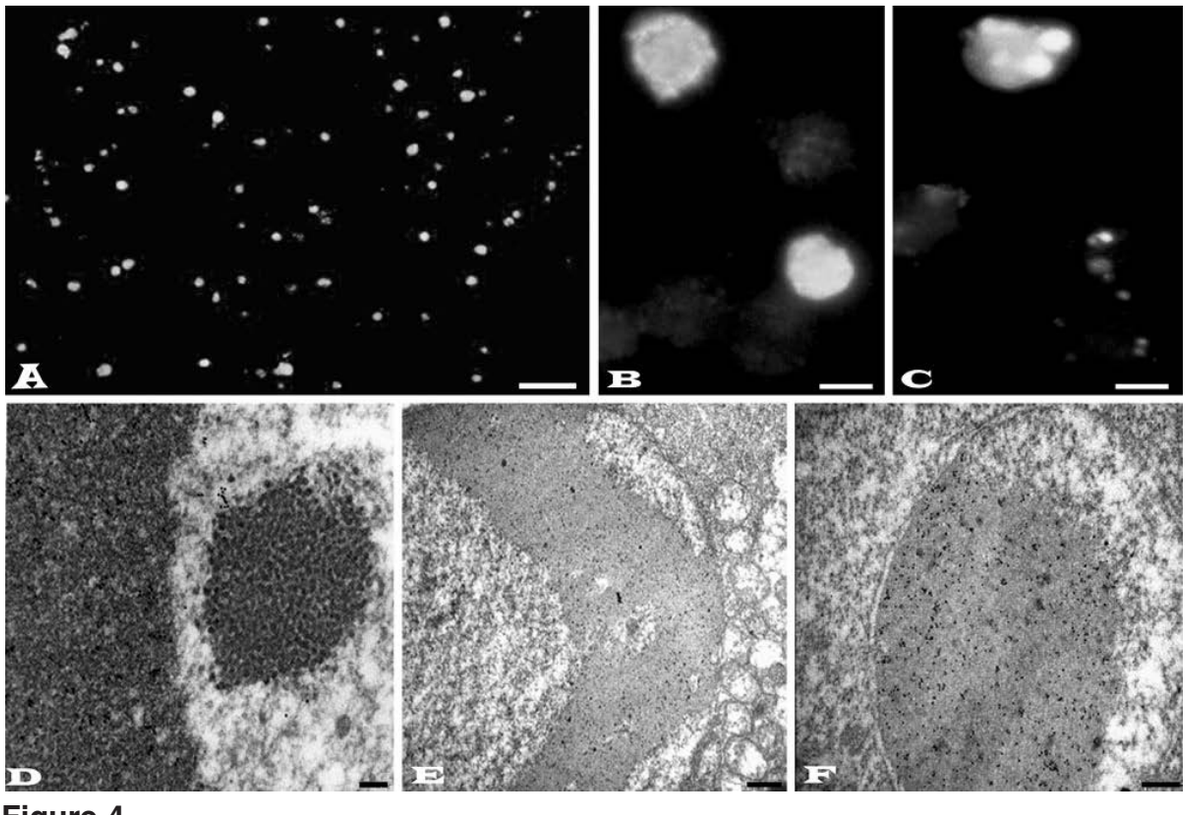

Figure 4

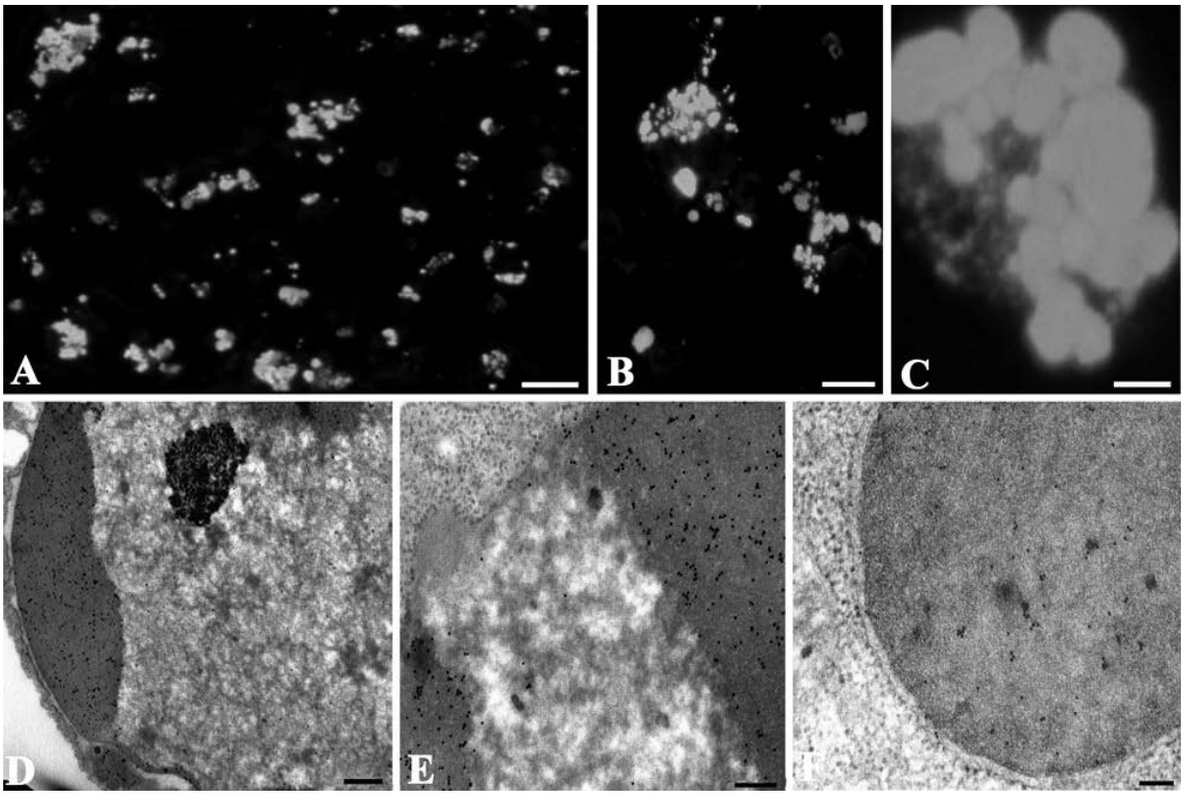

Figure 5. TUNEL/LM (A,B,C) and TUNEL/TEM (D-F) of U937 cells after staurosporine-treatment. Numerous fluorescent apoptotic cells (A), with strongly positive micronuclei (B,C), appear after TUNEL/LM. TUNEL/TEM positivity is less intense than that appearing after UVB-exposure. Gold particles are present in the dense chromatin and the micronuclei (C-E), but are more scarse in the diffuse one (E). Nucleolar components (D) and cytoplasm (E) appear negative. A bar=500 µm; B bar=25 µm; C bar=10 µm; D bar=0,5µm; E,F bar=0,2 µm

Figure 3. TUNEL/LM (A-C) and TUNEL/TEM (D-F) of U937 cells after UVB-exposure. A strong positivity (A-C), with fluorescent micronuclei (B,C), appears after TUNEL/LM. TUNEL/TEM reveals an intense colloidal gold particle labelling in the dense apoptotic chromatin, in contrast with the diffuse one, which appears weakly labelled (D,E) and shows negative nucleoli (D). Micronuclei appear very strongly labelled too (F). A bar=500 µm; B,C bar=25 µm; D,F bar=0,5 µm; E bar=1 µm

Figure 4. TUNEL/LM (A-C) and TUNEL/TEM (D-F) of Molt-4 cells after UVB-exposure. TUNEL/LM shows several positive cells (A-C). TUNEL/TEM reveals a gold particles number smaller than that of UVB-treated cells (Figure 4 D-F). Labelling is, again, rigorously present in the dense chromatin and in micronuclei (D-F) and rarely observable in the diffuse one (D-F), where nucleoli are negative (D). A bar=500 µm; B,C bar=25 µm; D bar=0,2 µm; E bar=1 µm; F bar=0,5 µm

(Figure 3 D). On the contrary, diffuse chromatin appears scarcely labelled (Figure 3 D,E).
Moreover, Figure 3D shows negative nucleoli, except for a weak labelling at their periphery.
Micronuclei present an intense labelling too (Figure 3 F).
Also UVB-treated Molt-4 appear positive at TUNEL/LM (Figure 4 A-C), but sensibly less fluorescent respect U937 cells in the same condition (Figure 3 A-C). TUNEL/TEM (Figure 4 D-F) reveals a smaller number of nuclear gold particles in comparison with UVB-treated U937 cells (Figure 4 D-F). Gold particles are present on dense chromatin and are rarely observable in the diffuse one (Figure 4 D, E) while the cytoplasm is negative (Figure 4 E).
In this cell line nucleoli are negative (Figure 4 D) and micronuclei appear diffusely labelled (Figure 4 F). A typical feature of chromatin rearrangement in Molt-4 apoptotic cells is the presence of negative diffuse chromatin spots surronded by positive areas. (Figure 4 E) [21].
Also staurosporine-treated U937 cells present apoptotic morphological features.
TUNEL/LM (Figure 5 A-C) reveals a lot of fluorescent apoptotic cells with highly positive micronuclei. TUNEL/TEM (Figure 5 D-F) shows an intense labelling, but more scarce than that revealed after UVB-exposure. Also in this experimental condition gold particles label is present in dense chromatin and micronuclei, much weaker in diffuse chromatin domains (Figure 5 E,F) and absent in the cytoplasm (Figure 5 E). Figure 5 D shows negative nucleolus and the positivity of dense chromatin.
Finally, staurosporine-treated Molt-4 cells (Figure 6) both by TUNEL/LM (Figure 6 A-C) and TUNEL/TEM (Figure 6 D-F) show an even lower positivity. Again we can observe the presence of micronuclei (Figure 6 C,F) and negative nucleolar components(Figure 6 D).
Dense chromatin appears labelled, while the diffuse one (Figure 6 D) and cytoplasm are negative

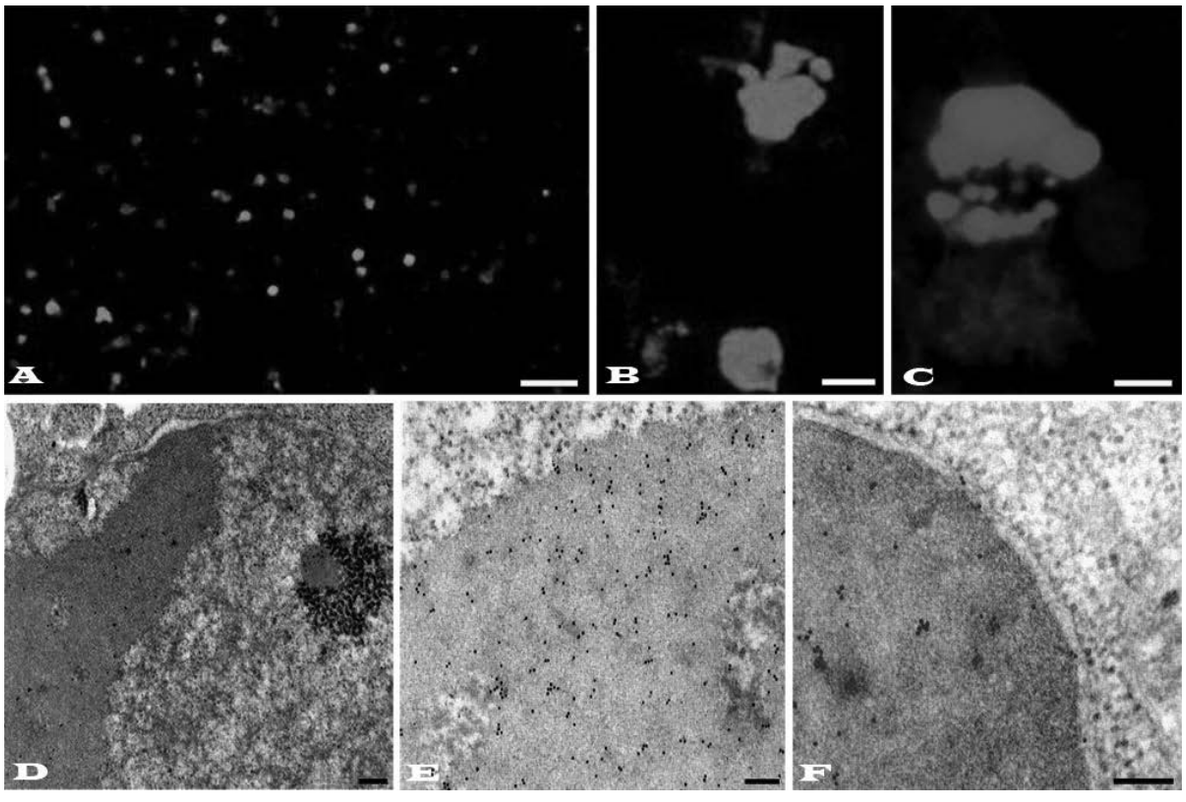

Figure 6. TUNEL/LM (A,B,C) and TUNEL/TEM (D-F) of staurosporine-treated Molt-4 cells. Both show a sensibly lower positivity. Gold particles are present in the dense chromatin (D-F) and, very scarcely, in the diffuse one (D,E). Nucleolar components (D), as well as cytoplasm (E) are consistently negative. A bar=500 µm; B bar=25 µm; C bar=10 µm; D,E,F bar=0,2 µm

(Figure 6 B).
The colloidal gold particle density was evaluated as above described and was expressed as gold particle number/μm². The statistical analysis confirmes the ultrastructural observations (Figure 7 A, B).

Discussion

A strong relationship exists between structural chromatin compacting and functional activity of cell nucleus [22].
Several studies have demonstrated that DNA fragmentation takes place in two steps: DNA is first cleaved into high molecular weight fragments of 300 and 50 Kbp which, succesively, these are furtherly reduced into smaller oligonucleosomes. This is typical of many, but not all, cell models [24-26].
In our study, we have induced apoptosis in U937 and in Molt-4, known to be very sensitive or relativly resistant, respectively.
By TUNEL/TEM, both U937 and Molt-4 appear, after UVB irradiation, strongly labelled on dense chromatin even if few gold particles appear on nuclear euchromatin of control cells. T
his is possible because, also in control cells DNA breaks, induced by DNA repair system, or site of active transcriptional genes can be revealed [26].
Nevertheless, UVB-treated U937 cells show a more intense labelling if compared to Molt-4: in fact they present the highest colloidal gold particle density, i.e. 350 μm². Molt-4 cells are 198/μm² (Figure 7).
Also staurosporine-treated U937 cells show the presence of particles in dense chromatin too, but with minor density, 271/μm² (Figure 7).

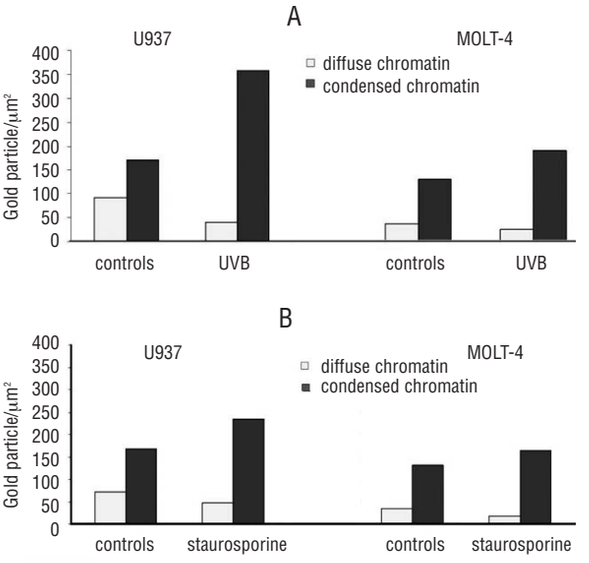

Figure 7. Histograms of colloidal gold particle density in diffuse and condensed apoptotic chromatin. A: control and UVB-treated U937 and Molt-4 cells. B: control and staurosporine-trated U937 and Molt-4 cells.

Molt-4 labelling at same condition appears even lower: 181/μm² (Figure 7).
DNA fragmentation can be so analysed not only by conventional or field inversion electrophoresis (data not shown), but also *in situ* by this modified TUNEL technique.
Gold particle density can be reasonably correlated to double strand break density, as well as, finally to DNA fragment lenght. Moreover, this technical approach allows the localization of DNA cleavage sites in apoptotic nuclear domains.

References

1. Zamai L, Burattini S, Luchetti F, et al. In vitro apoptotic cell death during erythroid differentiation. Apoptosis 2004;9: 235-246.
2. Movassagh M, Foo RS. Simplified apoptotic cascades. Heart Fail Rev. Dec 12, 2007; in press.
3. Falcieri E, Luchetti F, Burattini S, Canonico B, Santi S, Papa S Lineage-related sensitivity to apoptosis in human tumor cells undergoing hyperthermia. Histochem Cell Biol 2000;113:135-144.
4. Luchetti F, Mannello F, Canonico B, et al. Integrin and cytoskeleton behaviour in human neuroblastoma cells during hyperthermia-related apoptosis. Apoptosis 2004;9:635-648.
5. Rich T, Allen RL, Wyllie AH Defying death after DNA damage. Nature 2000;407:777-783
6. Solov'yan VT, Andreev IO, Kolotova TY, Pogribniy PV, Tarnavsky DT, Kunakh VA The cleavage of nuclear DNA into high molecular weight DNA fragments occurs not only during apoptosis but also accompanies changes in functional activity of the nonapoptotic cells. Exp Cell Res 1997;235:130-137.
7. Nagata S Apoptotic DNA fragmentation. Exp Cell

Res 2000;256:12-18.
8. Goping G, Wood KA, Sei Y, Pollard HB. Detection of fragmented DNA in apoptotic cells embedded in LR white: A combined histochemical (LM) and ultrastructural (EM) study. J Histochem Cytochem 1999;47:561-568.
9. Widlak P. The DFF40/CAD endonuclease and its role in apoptosis. Acta Biochim Pol 2000;47:1037-1044.
10. Marini M, Musiani D, Sestili P, Cantoni O Apoptosis of human lymphocytes in the absence or presence of internucleosomal DNA cleavage. Biochem Biophys Res Commun 1996;229: 910-915.
11. Kuribayashi N, Sakagami H, Iida M, Takeda M Chromatin structure and endonuclease sensitivity in human leukemic cell lines. Anticancer Res 1996;16: 1225-1230
12. Renò F, Burattini S, Rossi S, et al. Phospholipid rearrangement of apoptotic membrane does not depend on nuclear activity. Histochem Cell Biol 1998;110:467-476.
13. Iguki K, Hirano K, Ishida R Activation of caspase-3, proteolytic cleavage of DFF and no oligonucleosomal DNA fragmentation in apoptotic Molt-4 cells. J Biochem 2002;131:469-47.
14. Somosy Z.Radiation response of cell organelles. Micron 2000;31:165-81. Review.
15. Luchetti F, Burattini S, Ferri P, Papa S, Falcieri E Actin involvement in apoptotic chromatin changes of hemopoietic cells undergoing hyperthermia. Apoptosis 2002;7:143-152.
16. Sestili P, Martinelli C, Bravi G, et al. Creatine supplementation affords cytoprotection in oxidatively injured cultured mammalian cells via direct antioxidant activity. Free Radic Biol Med 2006;40:837-849
17. Luchetti F, Canonico B, Mannello F, et al. Melatonin reduces early changes in intramitochondrial cardiolipin during apoptosis in U937 cell line. Toxicol In Vitro 2007;21:293-301.
18. Burattini S, Ferri P, Battistelli M, Curci R, Luchetti F, Falcieri E C2C12 murine myoblasts as a model of skeletal muscle development: morpho-functional characterization. Eur J Histochem 2004;48:223-233.
19. Lossi L, Mioletti S, Merighi A Synapse-independent and synapse-dependent apoptosis of cerebellar granule cells in postnatal rabbits occur at two subsequent but partly overlapping developmental stages. Neuroscience 2002;112:509-523.
20. Hayashi R, Ito Y, Matsumoto K, Fujino Y, Otsuki Y Quantitative differentiation of both free 3'-OH and 5'-OH DNA ends between heat-induced apoptosis and necrosis. J Histochem Cytochem1998;46:1051-1059.
21. Vitale M, Zamai L, Falcieri E, et al. IMP dehydrogenase inhibitor, tiazofurin, induces apoptosis in K562 human erythroleukemia cells. Cytometry 1997;30: 61-66.
22. Andreev IO, Solovyan VT, Spiridonova KV, Kunakh VA Changes in a pattern of HMW-DNA fragmentation accompany differentiation and ageing of plant cells. BMC Plant Biology 2005;5(Suppl 1): S2
23. Bicknell GR, Snowden RT, Cohen GM Formation of high molecular mass DNA fragments is a marker of apoptosis in the human leukaemic cell line, U937. J Cell Sci 1994;107:2483-2489.
24. Huang P, Robertson LE, Wright S, Plunkett W High molecular weight DNA fragmentation: a critical event in nucleoside analogue-induced apoptosis in leukemia cells. Clin Cancer Res 1995;1:1005-1013.
25. Higuki Y. Glutathione depletion-induced chromosomal DNA fragmentation associated with apoptosis and necrosis J Cell Mol Med 2004;8:455-464.
26. Thiry M. In situ nick translation at the electron microscopic level: a tool for studying the location of DNAse I-sensitive regions within the cell. J Histochem Cytochem 1991;39:871-874.